ISSN 1990-3413, Astrophysical Bulletin, 2019, Vol. 74, No. 2, pp. 234–245. © Pleiades Publishing, Ltd., 2019.
Russian Text © The Author(s), 2019, published in Astrofizicheskii Byulleten', 2019, Vol. 74, No. 2, pp. 249–261.

Observations within the Framework of SETI Program on RATAN-600 Telescope in 2015 and 2016

A. D. Panov[1*], N. N. Bursov[2], G. M. Beskin[2,3], A. K. Erkenov[2], L. N. Filippova[4], V. V. Filippov[4], L. M. Gindilis[5], N. S. Kardashev[6], A. A. Kudryashova[2], E. S. Starikov[4], J. Wilson[7], and L. A. Pustilnik[8]

[1]*Skobeltsyn Institute of Nuclear Physics, Moscow State University, Moscow 119991 Russia*
[2]*Special Astrophysical Observatory, Russian Academy of Sciences, Nizhnii Arkhyz, 369167 Russia*
[3]*Kazan (Volga Region) Federal University, Kazan, 420008 Russia*
[4]*SETI Research and Cultural Center, Russian Academy of Cosmonautics, Moscow, 119991 Russia*
[5]*Sternberg Astronomical Institute, Moscow State University, Moscow, 119991 Russia*
[6]*Astro Space Center, Lebedev Physical Institute, Russian Academy of Sciences, Moscow, 117997 Russia*
[7]*SETI@HOME Project, New York, 14009 USA*
[8]*Tel Aviv University, Tel Aviv, 69978 Israel*

Received December 11, 2018; revised April 15, 2019; accepted April 15, 2019

Abstract—In 2015–2016 regular observations within the SETI program were carried out at the RATAN-600 radio telescope of the Special Astrophysical Observatory of the Russian Academy of Sciences. The aim of observations was to search for artificial signals from about 30 Sun-like stars and two metal-rich globular clusters. The main underlying idea of these studies was to perform multiple repeated observations (monitoring) of the same objects. The data were analyzed using three methods: we (1) searched for a strong single signal, (2) estimated the flux averaged over the entire observing time, and (3) analyzed the correlations between signals at different frequencies. Collecting the data over two observing years made it possible to perform a search for weak signals at the detection level of several mJy at 2.7 and 6.3 cm wavelengths. The power limits on the signals of extraterrestrial civilizations averaged over the entire data set lie in the 10^{16}–10^{20} W interval practically for all objects, whereas the upper luminosity limits for single observations (the beam crossing time was 7–19 s) are 10^{17}–10^{21} W and the effective isotropic emitted power of the hypothetical transmitters of the said civilizations do not exceed 2×10^9–2×10^{13} W, which is close to the corresponding parameter for the biggest planetary radars. The resulting luminosity limits are indicative of the absence of radio emission from the observed Sun-like stars, which is stationary on average and exhibits flare-like behavior during some observing sessions.

DOI: 10.1134/S1990341319020123

Key words: *SETI*

1. INTRODUCTION

The searches for signals from extraterrestrial civilizations (EC) have been performed over almost 60 years. Starting with the pioneering works of Cocconi and Morrison [1] and Drake [2], several thousand papers have been published on the subject in recent years, but no evidence has been found for the existence of extraterrestrial intelligence. The efficiency of the search is characterized by the investigated fraction of the volume of the multidimensional space of search parameters where measurements include the sensitivity of the detector, coordinates of the object, carrier frequency of the signal, the amplitude and temporal structure of the signal (period, duty ratio, etc.), frequency bandwidth, and polarization. The dimension of the space and the method used to estimate the volume studied vary depending on the prior ideas about the artificial signal and the strategy of its detection (see, e.g., [3–5]). The intensity of SETI studies has increased substantially in recent years owing to the "Breakthrough Initiatives" project [1], and this primarily happened at radio frequencies [6–8]. However, according to various estimates, the fraction

*E-mail: panov@dec1.sinp.msu.ru

[1] https://breakthroughinitiatives.org

of the investigated search parameter space volume lies in the interval from 5×10^{-26} to 1.5×10^{-18} with a geometric mean of 2.5×10^{-22} [4, 5]. (This analysis did not take into account the results of surveys [9, 10]. These very surveys demonstrated the absence of any beacons of type-II civilizations in the nearest region of the Galaxy (within 1 kpc). One may expect that taking the results of these surveys into account would change this estimate by about one order of magnitude.) Jill Tarter metaphorically commented the above figures [4]: "Coincidentally, the Earth's oceans hold 1.4×10^{18} m^3 of water, or 6×10^{21} cups of water. So our search of the 9-dimensional haystack is equivalent to sampling about 1.6 cups of water from the Earth's oceans. If you were looking for fish instead of extraterrestrial intelligence, I don't think that you would conclude that there are no fish in the ocean after this meager sampling!" These considerations inspire hope, but the estimates themselves are depressing—it is clear that no effort can increase them substantially. The only hope is to use information about places where "fish" concentrate, i.e., guide ourselves by the existing concepts of the origin of life and the possibility for it to reach intelligent (civilized) stage, and by modelling the strategy of establishing communication between ECs (see, e.g., [11]), thereby determining the search space domains with higher probability of finding extraterrestrial life and, possibly, civilization.

It is evident that such a domain naturally materialized after the discovery of exoplanets [12], and also as a result of the launch of the Kepler Space Telescope [13], which discovered several thousand planets orbiting other stars including several dozen Earth-like planets[2], located in the habitable zone [14]. These very stars are the primary objects in various SETI programs [8, 15–18]. Note that observations are usually performed at Gigahertz frequencies (the "water hole") [19] using the classical method proposed 50 years ago with a frequency resolution of 1–100 Hz with each object recorded once with a several-minutes long exposure (see, e.g., Enriquez et al. [8]). This approach is based on the idea that a transmission from an extraterrestrial civilization should have the form of narrow-band emission (untypical for astrophysical objects) preceding the message proper, which should be transmitted after the link is established (i.e., when an answer—"a ready signal" is sent from the Earth) [11]. Note that this is why the rare cases of the detection of single radio bursts of inexplicable origin, e.g., the famous "WOW!" signal, created such great excitement.

[2] http://phl.upr.edu/projects/habitable-exoplanets-catalog

The recently accumulated data allow us to upgrade in a particular way our concepts about the possible nature of transmissions and broadcasts by extraterrestrial civilizations, and hence to alter the strategy of their search. This study is dedicated to the implementation of one of the versions of modified search strategy.

2. BASIC PREREQUISITES OF THE STRATEGY OF THE SEARCH FOR SIGNALS FROM EXTRATERRESTRIAL CIVILIZATIONS

First, it is time to recognize that no dialog between civilizations is possible. The most optimistic estimates of the number of civilizations based on the results of the investigation of exoplanets (including Earth-like worlds) and our concepts about the duration of the technological stage, imply that the neighboring civilizations should be 500–1000 pc apart [20]. On the other hand, even just the planets that are most suitable for the emergence of life are mostly located at a distance of 10–50 pc from the Sun. It follows from this that transmission should include all the information meant for us, i.e., the volume of the message should be maximal. According to the Shannon–Hartly theorem (see [21]), the throughput of a communication channel is proportional to the frequency bandwidth, i.e., if an EC plans to broadcast in the no-feedback mode, it should use broadband signals. It is clear that in this case such a civilization should use directional antennas whose beams periodically (repeatedly) cross target objects [22]. A fundamental point of this strategy is the repeated irradiation of the target object of the message required to increase the probability of the extraterrestrial signal to be detected by this target object. In other words, we must conduct repeatedly our observations of possible sources of artificial radiation hoping to capture the time (period) of the transmission. As for the criterion of artificialness of the signal, it may be its complex (nonstandard, nonperiodic) temporal structure. Such a method of coding seems to be more simple and natural compared to all sorts of variations of frequency and polarization. It can be observed that the objects of the search for EC transmissions are either Earth-like planets or their associated beacons and, therefore, the effects of the blurring of the temporal (and, evidently, also the frequency) structure should be insignificant [15, 23]. In particular, with a dispersion measure of 100–200 pc cm^{-3}, carrier wavelength of 6 cm, and frequency bandwidth of 1 GHz, the temporal broadening of the signal does not exceed 10^{-5}–10^{-4} s.

In this paper, which partially implements the above strategy, we report the results of multiple

RATAN-600 cm-wavelength observations made in 2015–2016 for a sample of Sun-like stars with exoplanets. Within the framework of this program, we also performed another task—we searched for variable radio emission from the same stars due to their flare activity. Note that optical superflares detected by the "Kepler" space telescope [24] may be accompanied by variable radio emission of nonthermal particles. The latter, in turn, may have a significant effect on the possibility of the emergence and preservation of life (including intelligent life) on planets orbiting these stars [25].

Let us now discuss in more detail the underlying ideas of the program for search for signals from ECs. It can be assumed that if some cosmic civilization has serious intention to interstellar communication then it can over a very short time scale (in historical or astronomical terms) build sufficiently powerful multifrequency transmitters to broadcast interstellar messages. However, if a civilization does not have energy resources comparable in power to the luminosity of their own parent star (in other words, it is the first-type civilization in accordance with Kardashev's classification [26]), it cannot transmit a sufficiently powerful signal in all directions at the same time due to fundamental energy restrictions. Hence, if we talk about sufficiently powerful signals like those of a beacon, which can be easily detected by other civilizations, then a civilization of the first type can only scan the space the star after star. Any recipient of such signals can expect to detect only relatively short signal portions separated by long periods of silence. If only Kardashev's type-2 civilizations (those that have mastered energy at the level of their parent star) are not very widespread in our Galaxy, then, generally speaking, one should not expect continuous interstellar messages with high signal power from candidate SETI stars. Therefore, if someone has observed a certain SETI candidate star, even very thoroughly and using high sensitivity tools, but only once, and has detected no artificial signals, then it cannot be concluded from this that the star in question is not inhabited by a communicative civilization. This star can start broadcasting toward the Solar system just at the time when the observer's attention switches to another SETI candidate star. Nondetection of a signal from a star after a single observation effectively provides no information about this star assuming that we are looking for a type-1 civilization.

It is clear from the above that the ideal SETI strategy is to continuously monitor each SETI candidate or to simultaneously perform continuous observations in all directions (preferably over a broad frequency range and searching for different types of signal modulation). Unfortunately, this is not yet possible, assuming a sufficiently high sensitivity of the receiver. A reasonable compromise is to periodically monitor—as frequently as possible—a limited list of SETI candidates.

The main idea underlying the program implemented at the RATAN-600 radio telescope was to periodically monitor a limited number of objects over a long period of time. In this way, the maximum duration of a single message for each candidate can be limited: the maximum duration of a message cannot exceed the maximum time gap between successive observations of the SETI candidate. Another advantage of the program is that it allows accumulating the signal of many successive observations of the same object and eventually find weak signals that are below the detection limit for a single observation.

3. TECHNIQUE

The observations were carried out on the Southern sector of the annular antenna of RATAN-600 radio telescope with a flat reflector and the "Feeder No. 2" receiving-and-measuring facility of the secondary mirror. In this case, a three-mirror scheme was used, where the flat reflector played the role of the main receiving mirror, and the elements of the sectors of the ring antenna were installed vertically and fixed. The advantage of this scheme is that it makes it possible to quickly repoint the flat sector of the antenna allowing 80-90 sources per day to be observed. The disadvantages of such a scheme are, first, the loss (dissipation) of energy at the surfaces of the mirrors, especially at short waves, and due to inaccurate alignment of the foci; and second, relatively strong aberrations at the edges of the visual field. In such a system, the ground radiation contributes relatively strongly to the background, resulting in about a factor-of-two loss of sensitivity with respect to the observation mode with individual sectors of the telescope, especially for high elevation angles. Observations were carried out with the "Eridan-2" radiometer at three regular frequencies. After a deep upgrade of the outdated and inefficient nitrogen cooling system, the facility now consists of a set of warm (uncooled) radiometers [27] with the characteristics presented in Table 1.

The 2.7- and 6.3-cm radiometers operated without losses and had maximum sensitivity (compared to the sensitivity at 1.38 cm). Because of this, we reduced only the data acquired with these two radiometers operated in the broadband mode (see Table 1).

The data reduction was carried out using standard FADPS software [28]. We used the calibration sources 0137+33 (3C 48), 0237−23, 0521+16 (3C 138), 0542+49 (3C 147), 0627−05 (3C 161), 1154−35, 1256−05, 1331+30 (3C 286), 1347+12, 1411+52 (3C 295), 1459+71 (3C 309.1), 1850−01,

Table 1. Basic characteristics of "Eridan-2" radiometers

Characteristics of radiometers	Wavelength		
	1.4 cm	2.7 cm	6.3 cm
Noise temperature, K	185	100	60
Bandwidth, GHz	2.5	0.8	0.6
Expected sensitivity for 1 s long observation, mK	6.0	5.0	3.5
Transit time for a point source[a], s	4–5	7–9	12–19

[a] Telescope beam size at zero power level with allowance for aberrations. The value in the interval is determined by the declination of the source.

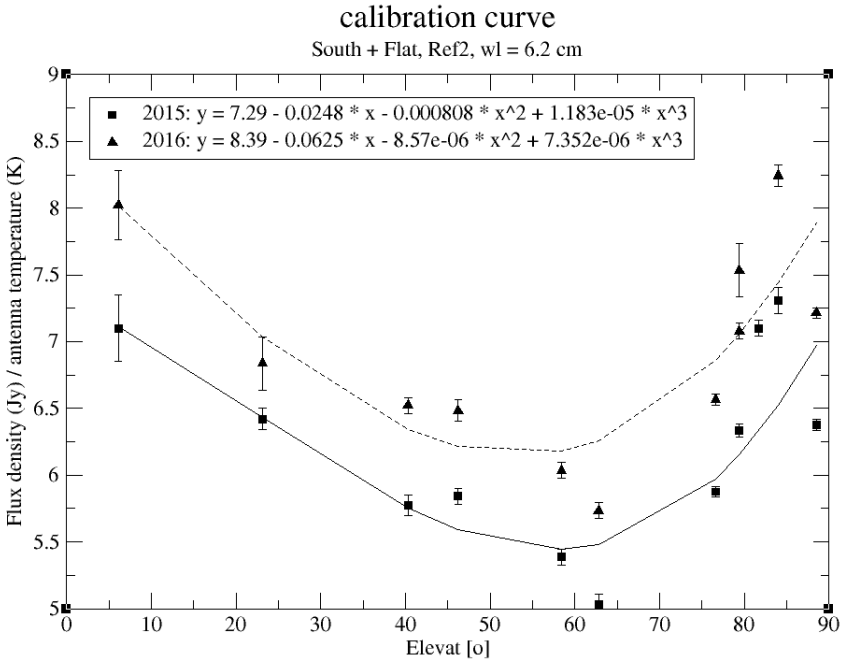

Fig. 1. Calibration curves for transforming antenna temperatures into 6.2-cm fluxes for the Southern sector of the telescope with a flat mirror in 2015 (the solid line) and 2016 (the dashed line).

and 2107+42 (NGC 7027) representing the entire visible sky to construct the curves for correcting the right ascension and transform the antenna temperatures into fluxes for the 2.7- and 6.2-cm wavelengths.

Conversion of the amplitudes of signal sources expressed in terms of antenna temperatures at the radio telescope output to the flux densities of radio emission sources in mJy was carried out using data from calibration sources based on two years of observations with the Southern sector with a flat reflector. Figure 1 shows calibration curves for converting antenna temperatures into fluxes at a wavelength of 6.2 cm. Calibration is not completely time independent and was conducted separately for the 2015 and 2016 observations. We fitted the experimental calibration curves to cubic polynomials, as shown in Fig. 1.

4. LIMITED LIST OF SETI CANDIDATES AND STATISTICS OF OBSERVATIONS

We used the following criteria for including objects into the limited list of SETI candidates for monitoring:

- Sun-like stars with known planets (the number of planets is given in parentheses): HD 1461 (2+2?), HD 10700 (5?), HD 13931 (1), HD 38858 (1), HD 45184 (1), HD 69830 (3), HAT-P-43 (1), HD 75732 (5), HD 89307 (1), HD 95128 (3),

HD 134987 (2), HD 150433 (1), HD 154088 (1), HD 164595 (1), CoRoT-9 (1), Kepler-69 (2), Kepler-452 (1);

- Sun-like planets close to the ecliptic: HD 50692, HD 99491, HD 154088, HD 172051 [29];
- Stars-recipients of the first radio messages from the Earth: HD 50692, HD 75732, HD 95128, HD 186408, HD 197076;
- Metal-rich globular clusters NGC 6553 and PAL 10 ([Fe/H] = −0.18 and −0.10, respectively). This metallicity level is close both to the solar metallicity and the metallicities of many stars with already discovered planets. The distances to these globular clusters are equal to 19 000 and 20 000 light years, respectively.

Table 2 lists the basic properties of the stars and planets in the list. The columns give the following information: (1)—name of the star, mostly according to the HD Catalog [30]; (2)—spectral type; (3)—apparent magnitude of the central star; (4)—distance to the star; (5)—mass of the star in solar masses; (6)—radius of the star in solar radii; (7)—temperature of the star; (8)—metallicity of the star; (9)—age of the star in Gyr; (10)—number of the planet (a,b,c,...), the METI (Messaging for Extra Terrestrial Intelligence) is also given here if the star was a target of terrestrial interstellar communications, and (11)—the mass of the planets in Jupiter masses (M_j). The mass is determined as $M\sin(i)$, if the planet was discovered using the radial-velocity method; here i is the inclination of the orbital plane of the planet to the line of sight (unknown). Letter M printed next to the mass means that the mass was determined using a different method. (12)—the orbital period around the star in days.

The basic properties of globular clusters, like those of the stars, are adopted from astronomical databases [31, 32], exoplanet databases, and other Internet resources [33–38].

RATAN-600 radio telescope operates in the transit mode. This means that each object can be observed only once a day when it crosses the telescope beam. The approximate transit time for different wavelengths is listed in the last row of Table 1. The total duration of a single transit record in the vicinity of the record center was typically equal to 2.5 min.

Table 3 lists all observed objects, the coordinates of each object, the number of transits through the telescope beam (the number of days the object was observed), the total signal integration time computed as $t_{\rm sum} = t_{\rm ndays} \times t_{\rm obs}$, where $t_{\rm ndays}$ is the number of days the object was observed and $t_{\rm obs}$, the total time of one observation. The globular cluster PAL 10 was observed only ten times in 2015 and was not observed at all in 2016 and we therefore did not include it into the tables.

5. RESULTS AND DISCUSSION

Fig. 2 shows 65 transit curves of the calibrating point source 0542+16 (3C 138) at 2.7 cm. The records were obtained after applying the correction for the uncertainty of the feeder position when it moves along the rails and the correction for the amplitude due to the variation of the effective area of the antenna sector and variations of the gain of radiometers. The correction curves were obtained from observations of bright sources within the framework of other programs in 2015 and 2016. The profiles of the lines reproduce the shape of the beam of RATAN-600 radio telescope.

The trace of the side lobe of the beam can be seen left of the main peak. It is expected that an artificial source should exhibit a similar signal shape. If the signal is sufficiently strong then it can be detected on a single record of the object's transit above the background surrounding the peak. No peaks matching the expected shape of the signal of a point source were found in the single records of SETI candidates from the limited list recorded during two years of observations.

As we pointed out above, if the signal from a source exists, but is too weak to be detected in a single measurement, it can still be detected after integration over several records. The integration method was implemented off-line during data reduction.

When searching for weak signals using the integration method we subdivided all records of SETI candidates after performing the necessary primary reduction (separately for each candidate) into two groups Sum1 and Sum2 so that the noise in the background poart of the record (where the true source signal should not appear) would be the same in each group. For each group we used the Hodges–Lehmann method [39] to determine the averaged signals and compute the following their combinations: Sum = (Sum1 + Sum2)/2 and Dif = (Sum1 − Sum2)/2.

If the measurements were made correctly and the possible signal did not depend on time than Sum should be equal to the sum of the signal and noise, and Dif to the pure noise. We tested this hypothesis to control the correctness of the measurement procedure and identify eventual anomalies in it.

To illustrate this, we show in Fig. 3 the estimates of Sum and Dif for two years of integration (182 records) for the source HD 150433 separately for the 2015 and 2016 data and separately for the 2.7 and 6.3-cm wavelengths. As is evident from the

Table 2. Properties of stars and planets from the limited list of candidate SETI objects of the study performed with RATAN-600 radio telescope

Star	Spectral class	V_{mag}, m	Distance to the star, pc	M, $M_\odot$	R, $R_\odot$	T, K	Fe/H	Age, Gyr	No. Planets	M, M_j	P, days
(1)	(2)	(3)	(4)	(5)	(6)	(7)	(8)	(9)	(10)	(11)	(12)
HD 1388	G0V	6.50	26.1	1.18	1.11	5952	−0.04	5.6	?	?	
HD 1461	G0V	6.64	23.4	1.14	1.1	5765	0.19	6.3	b	6.9	5.77
									c	5.9	13.5
HD 13931	G0	7.61	45.5	1.04	1.23	5868	0.03	6.4	b	1.88	4218
HD 38858	G2V	5.97	15.2	1.05	0.93	5723	0.21	7.5	b	0.09	407
CoRoT-5	F9V	14	400	1.00	1.19	6100	0.25	6.9	b	0.46	4.04
HD 50692	G0V	5.74	17.3	0.98	1.08	5891	0.13	5.5	METI		
HD 51419	G5V	6.94	24.2	1.0	0.97	5637	0.33	4.8			
HD 69830	G8V	5.95	12.6	0.86	0.91	5385	0.05	7.0	b	10.2	8.67
									c	11.8	31.6
									d	18.1	197
HAT-P-43	G	13.36	543	1.05	1.10	5645	0.23	5.7	b	0.66	3.33
HD 75732	G8V	5.95	12.34	0.95	0.94	5196	0.2	7.4	b	0.824	14.65
									c	0.169	44.34
									d	3.835	5218
									e	0.025	0.737
									f	0.144	260.7
HD 89307	G0V	7.06	30.9	1.03	1.05	5950	0.14	6.76	b	2	2199
HD 95128	G0V	5.1	13.97	1.08	1.22	5887	0.02	5.5	b, METI	2.53	1078
									c	0.54	2391
									d	1.64	10000
HD 99492	K2V	7.38	18	0.83	0.96	4740	0.36	4.0	b	0.11	17.04
HD 114783	K0	7.57	20.4	0.92	0.78	5105	0.33	7.8	b	1.1	493.7
HD 134987	G5V	6.45	22.2	1.07	1.25	5740	0.25	4.4	b	1.59	258.2
									c	0.82	5000
HD 146233	G2V	5.50	14.0	0.98	1.02	5800	0.05	4.7			
HD 150433	G0	7.22	29.6	0.91	1.04	5649	0.22	5.0	b	0.168	1096
HD 154088	K01V	6.58	18.1	0.93	0.94	5409	0.28	6.4	b	0.019	18.6
HD 157347	G3V	6.28	19.5	1.19	1.02	5714	0.03	5.8			
HD 164595	G2V	7.1	28.93	0.99	1.04	5790	0.04	6.3	b	0.052	40
HD 164922	G9V	6.99	22.1	0.95	0.93	5467	0.16	5.2	b	0.34	1201
									c	0.041	75.76
HD 172051	G6V	5.86	13.0	0.93	0.89	5564	0.24	7.9			
CoRoT-25	G0V	15.0	1000	1.09	1.19	6040	0.01	5.2	b	0.27M	4.86
CoRoT-9	G3V	13.7	560	0.99	0.94	5625	0.01	4.0	b	0.84M	95.27
Kepler-69	G4V	13.7	830	0.81	0.93	5638	−0.2	5.8	b	0.67M	3.234
HD 186408	G1.5V	5.99	21.6	1.25	1.25	5781	0.08	5.8	METI		
HD 197076	G5V	6.44	21.0	1.00	0.98	5823	0.09	5.2	METI		
HD 217877	G0V	6.68	30.8	1.05	1.22	5953	0.10	4.2			

Table 3. List of SETI candidates and statistics of their observations in 2015–2016

Star	R.A. (J2000), hh:mm:ss	Dec. (J2000), dd:mm:ss	Number days	Time of observations, s	Name in observations
HD 1388	00 : 17 : 58.87	−13 : 27 : 20.3	51	658	0017 − 13
HD 1461	00 : 18 : 41.86	−08 : 03 : 10.8	71	902	0018 − 08
HD 13931	02 : 16 : 47.37	+43 : 46 : 22.7	31	530	0216 + 43
HD 38858	05 : 48 : 34.94	−04 : 05 : 40.7	50	635	0548 − 04
CoRoT-5	06 : 45 : 06.54	+00 : 48 : 54.8	103	1308	0645 + 00
HD 50692	06 : 55 : 18.66	+25 : 22 : 32.5	9	124	0655 + 25
HD 51419	06 : 58 : 11.75	+22 : 28 : 33.2	17	231	0658 + 22
HD 69830	08 : 18 : 23.94	−12 : 37 : 55.8	27	348	0818 − 12
HAT-P-43	08 : 35 : 42.17	+10 : 12 : 23.9	27	348	0835 + 10
HD 75732	08 : 52 : 35.81	+28 : 19 : 50.9	34	483	0852 + 28
HD 89307	10 : 18 : 21.28	+12 : 37 : 15.9	82	1058	1018 + 12
HD 95128	10 : 59 : 27.97	+40 : 25 : 48.9	41	664	1059 + 40
HD 99492	11 : 26 : 45.28	+03 : 00 : 22.2	8	102	1126 + 03
HD 114783	13 : 12 : 43.78	−02 : 15 : 54.1	45	572	1312 − 02
HD 134987	15 : 13 : 28.66	−25 : 18 : 33.6	53	726	1513 − 25
HD 146233	16 : 15 : 37.26	−08 : 22 : 09.0	179	2273	1615 − 08
HD 150433	16 : 41 : 08.21	−02 : 51 : 26.2	176	2235	1641 − 02
HD 154088	17 : 04 : 27.84	−28 : 34 : 57.6	118	1664	1704 − 28
HD 157347	17 : 22 : 51.28	−02 : 23 : 17.4	181	2299	1722 − 02
HD 164595	18 : 00 : 38.89	+29 : 34 : 18.9	204	2917	1800 + 29
HD 164922	18 : 02 : 30.86	+26 : 18 : 46.8	35	486	1802 + 26
HD 172051	18 : 38 : 53.40	−21 : 03 : 06.7	93	1237	1838 − 21
CoRoT-25	18 : 42 : 31.11	+06 : 30 : 49.7	126	1613	1842 + 06
CoRoT-9	18 : 43 : 08.81	+06 : 12 : 14.8	146	1854	1843 + 06
Kepler-69	19 : 33 : 02.62	+44 : 52 : 08.0	103	1792	1933 + 44
HD 186408	19 : 41 : 48.95	+50 : 31 : 30.2	97	1862	1941 + 50
HD 197076	20 : 40 : 45.14	+19 : 56 : 07.9	272	3645	2040 + 19
HD 217877	23 : 03 : 57.27	−04 : 47 : 41.4	54	686	2303 − 04
NGC 6553[b]	18 : 09 : 15.68	−25 : 54 : 27.9	35	483	1809 − 25

[b] Globular cluster

figure, the Dif function indeed does not deviate from purely noise behavior, but the Sum quantity exhibits signs of two statistically significant peaks, which correspond to two known off-axis radio sources J164039−023942 (350–500 mJy) and J164116−025027 (about 50 mJy) from the NVSS catalog [40, 41]. The signals are smoothed with the profile corresponding to the antenna beam. The expected position of the SETI candidate signal is denoted by the arrow. However, as is evident from

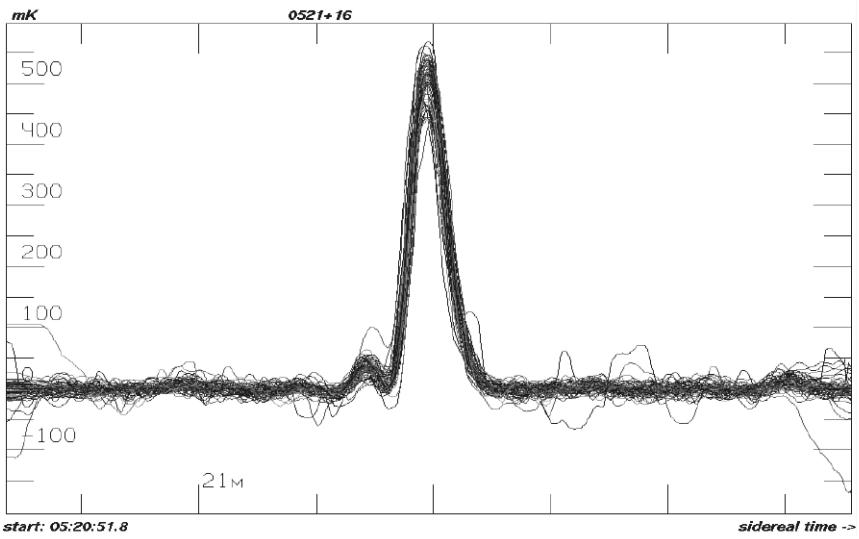

Fig. 2. 65 records of the beam transits for the calibrating source 0521+16 (the 3C 138 quasar with the coordinates: R.A.: 05:21:9.89, Dec.: 16:38:22.10 (J2000)). The tick step along the time scale is equal to 5 s.

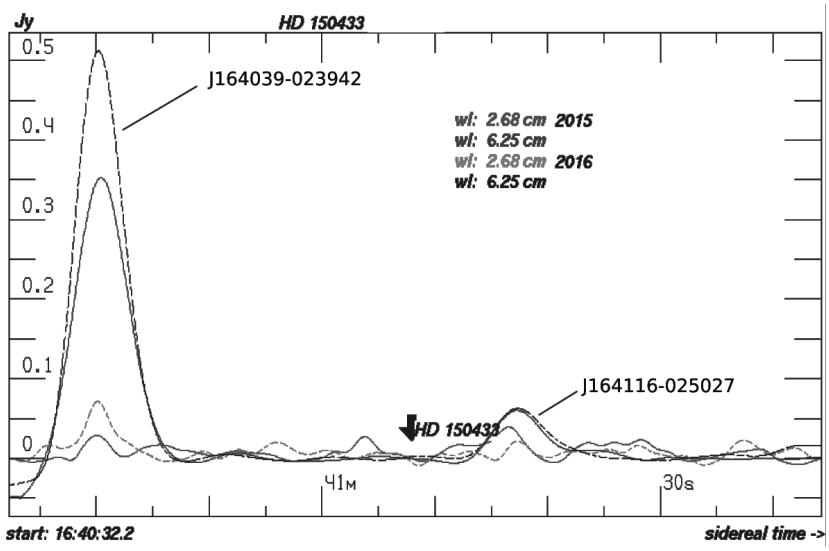

Fig. 3. Results of the signal accumulation for the source HD 150433 (1641 − 02) in 2015 (the solid line) and 2016 (the dashed line) separately for the 2.7 and 6.3 cm wavelengths after folding with the computed beam.

the figure, no signal signs can be seen at the expected position of the HD 150433 source.

Fig. 4 shows the signals for the HD 150433 candidate (1641−02) accumulated over the entire observing time in 2015 and 2016. Again, it is evident from the figure that the data contain no significant signal toward the SETI candidate.

We performed a similar analysis for each candidate. The known noise level allowed us to estimate the upper signal limit for each source. Table 4 lists these data for all objects of the limited SETI list for the significance level corresponding to three standard deviations. The same table lists the upper power limits for the signals averaged over all observing time and the corresponding quantities for a mean single observation (the second row in Table 4).

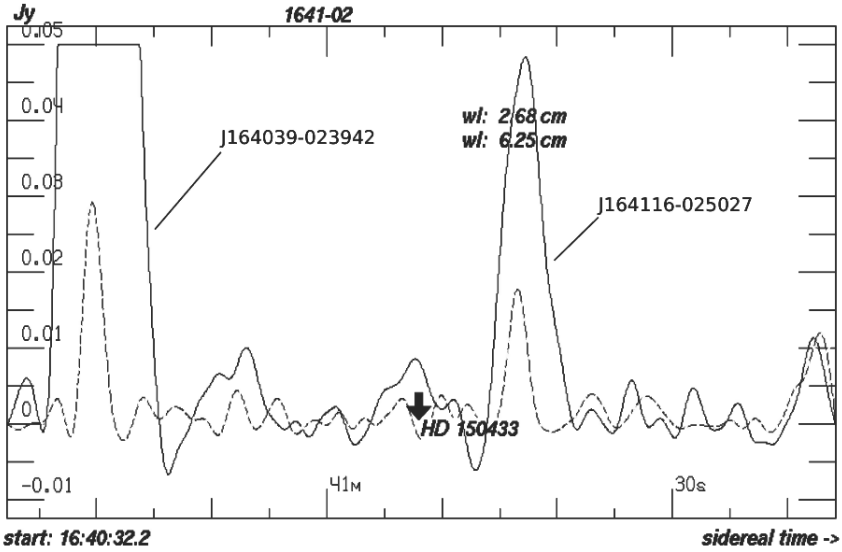

Fig. 4. Combined signal for the source HD 150433 (1641 − 02) over two years of observations (separately for the 2.7 and 6.3 cm wavelengths) after folding with the computed beam.

Table 4. Upper flux limits in mJy/signal power in W averaged over the entire observing period (the second row shows the average limits for flux/power of single-observation signals) for the candidates from the limited SETI list

Star	2015	2015	2016	2016	Name
	2.7 cm	6.3 cm	2.7 cm	6.3 cm	in observations
(1)	(2)	(3)	(4)	(5)	(6)
HD 1388	3/2.3e+17	7/4.6e+17	2/1.2e+17	2/1.1e+17	0017 − 13
	13/1.1e+18	22/1.4e+18	19/1.5e+18	21/1.4e+18	
HD 1461	28/1.8e+18	2/1.3e+17	35/2.3e+18	3/1.4e+17	0018 − 08
	91/6e+18	19/1e+18	233/1.5e+19	17/8.9e+17	
HD 13931	6/1.6e+18	41/8e+18	10/2.6e+18	23/4.6e+18	0216 + 43
	21/5.2e+18	50/9.9e+18	28/6.9e+18	51/1e+19	
HD 38858	12/3.3e+17	3/7.3e+16	6/1.8e+17	4/9.3e+16	0548 − 04
	34/9.4e+17	21/4.6e+17	51/1.4e+18	19/4.2e+17	
CoRoT-5	2/3.3e+19	3/5.1e+19	2/4.2e+19	3/5.1e+19	0645 + 00
	15/2.9e+20	20/3.1e+20	19/3.6e+20	19/2.9e+20	
HD 50692	5/1.7e+17	8/2.1e+17	4/1.6e+17	4/1.1e+17	0655 + 25
	15/5.4e+17	21/6e+17	17/6.1e+17	8/2.3e+17	
HD 51419	4/2.9e+17	25/1.4e+18	8/5.6e+17	12/6.4e+17	0658 + 22
	14/9.8e+17	28/1.6e+18	19/1.3e+18	17/9.5e+17	
HD 69830	6/1.2e+17	2/2.9e+16	2/4.6e+16	2/3.2e+16	0818 − 12
	13/2.5e+17	17/2.6e+17	16/3e+17	12/1.8e+17	
HAT-P-43	4/1.3e+20	4/1.2e+20	2/5.6e+19	4/1.3e+20	0835 + 10
	11/3.9e+20	16/4.5e+20	14/4.9e+20	15/4.2e+20	
HD 75732	3/5.4e+16	7/1e+17	3/5.1e+16	4/5.2e+16	0852 + 28
	14/2.5e+17	17/2.5e+17	18/3.3e+17	16/2.3e+17	
HD 89307	2/1.8e+17	2/1.6e+17	3/3.2e+17	3/2.6e+17	1018 + 12

Table 4. (Continued)

Star	2015	2015	2016	2016	Name
	2.7 cm	6.3 cm	2.7 cm	6.3 cm	in observations
(1)	(2)	(3)	(4)	(5)	(6)
	13/1.5e+18	18/1.6e+18	18/2.1e+18	19/1.7e+18	
HD 95128	4/9.9e+16	8/1.5e+17	7/1.6e+17	10/1.8e+17	1059 + 40
	15/3.5e+17	23/4.3e+17	28/6.5e+17	36/6.7e+17	
HD 99492	3/1e+17	7/2.2e+17	5/1.8e+17	4/1.2e+17	1126 + 03
	10/3.9e+17	15/4.7e+17	13/5e+17	6/1.9e+17	
HD 114783	7/3.6e+17	3/1.2e+17	3/1.7e+17	4/1.4e+17	1312 − 02
	16/8e+17	15/6e+17	20/1e+18	24/9.6e+17	
HD 134987	5/2.8e+17	5/2.4e+17	4/2.2e+17	7/3.4e+17	1513 − 25
	18/1.1e+18	20/9.4e+17	24/1.4e+18	32/1.5e+18	
HD 146233	8/2e+17	3/5.3e+16	6/1.4e+17	2/4.5e+16	1615 − 08
	67/1.6e+18	18/3.4e+17	130/3e+18	22/4.1e+17	
HD 150433	3/3e+17	3/2.3e+17	2/2.4e+17	5/4.4e+17	1641 − 02
	19/2e+18	19/1.6e+18	25/2.6e+18	23/1.9e+18	
HD 154088	4/1.5e+17	2/5e+16	4/1.6e+17	3/1e+17	1704 − 28
	22/8.6e+17	22/6.9e+17	22/8.6e+17	27/8.5e+17	
HD 157347	4/1.6e+17	2/6.2e+16	2/8.6e+16	1/4.7e+16	1722 − 02
	20/9.1e+17	16/5.8e+17	24/1.1e+18	23/8.4e+17	
HD 164595	1/1.3e+17	4/3.6e+17	2/1.5e+17	1/8e+16	1800 + 29
	17/1.7e+18	25/2e+18	22/2.2e+18	23/1.8e+18	
HD 164922	3/1.8e+17	11/5e+17	3/1.8e+17	16/7.6e+17	1802 + 26
	20/1.2e+18	26/1.2e+18	19/1.1e+18	34/1.6e+18	
HD 172051	2/4.2e+16	2/2.6e+16	1/2.6e+16	6/1e+17	1842 + 06
	16/3.2e+17	18/2.9e+17	21/4.2e+17	25/4e+17	
CoRoT-25	3/4.1e+20	4/3.9e+20	1/1.7e+20	2/2e+20	1843 + 06
	14/1.7e+21	18/1.7e+21	17/2e+21	20/1.9e+21	
CoRoT-9	1/3.3e+19	1/2.8e+19	2/5.6e+19	2/3.8e+19	1933 + 44
	15/3.8e+20	18/3.6e+20	18/4.6e+20	19/3.8e+20	
Kepler-69	5/4.1e+20	7/4.5e+20	4/3.7e+20	6/3.9e+20	1941 + 50
	25/2.1e+21	32/2.1e+21	31/2.6e+21	47/3.1e+21	
HD 186408	30/1.7e+18	212/9.5e+18	42/2.3e+18	130/5.8e+18	2040 + 19
	43/2.4e+18	215/9.6e+18	56/3.1e+18	143/6.4e+18	
HD 197076	1/7.4e+16	2/7.6e+16	1/5.8e+16	1/5.1e+16	2303 − 04
	15/7.9e+17	19/8e+17	19/1e+18	21/8.9e+17	
HD 217877	5/5.2e+17	5/4.4e+17	11/1.3e+18	3/2.8e+17	1809 − 25
	30/3.4e+18	17/1.5e+18	70/7.9e+18	21/1.9e+18	
NGC 6553	9/3.9e+22	5/1.8e+22	3/1.2e+22	10/3.3e+22	1838 − 21
	25/1.1e+23	20/6.9e+22	22/9.5e+22	39/1.3e+23	

Another method of searching for the broadband signal of SETI candidates consisted in searching for correlations between signals at the wavelengths of 2.7 cm and 6.3 cm. To determine the correlation

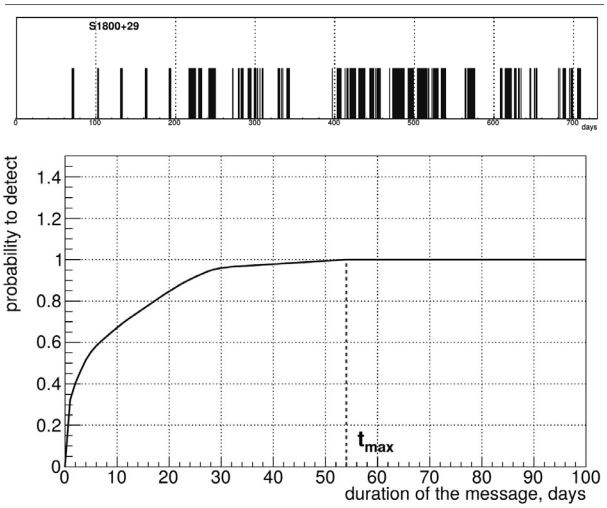

Fig. 5. Top panel: sequence of observations for the candidate 1800+29 (HD 164595). Bottom panel: probability of detection for a message from the same source depending on its duration. The dashed line in the plot shows the maximum signal duration $t_{\max}$ after which the detection probability becomes equal to 100%.

coefficients, we cross-matched the data sets of different wavelengths of each candidate by the observation time. The differences between the number of days of observation for different wavelengths are mainly due to too large external noise, which occurred independently at different frequencies, and sometimes due to the inoperability of a radiometer of some wavelength.

We computed the linear correlation coefficients between the 2.7 cm and 6.3 cm data sets for all candidates of the limited list. To control the randomness of correlations, we also applied a similar data processing procedure to the time series shifted of one, two, and three days. In all cases, the mean correlation coefficient was $r_{\rm avr} = 0.06 \pm 0.12$. This is indicative of the absence of non-random correlations between signals at different wavelengths. This is especially obvious for candidates with a large number of observations. Thus the correlation analysis also shows the absence of real signals for SETI candidates from the limited list.

As we already pointed out in the Introduction, for each SETI candidate constraints on the maximum duration of a single message can be obtained using a series of repeated observations. Fig. 5 (the top panel) shows the sequence of observations within the framework of one of the candidates' programs for the two-year period. It is evident from the figure that a signal with a power at the upper limit level from Table 4 would be detected with a probability of 100% provided that the broadcast duration exceeds 54 days.

For shorter messages their detection probability can be found. Fig. 5 (the bottom panel) shows the dependence of the detection probability of a message on its duration. It is evident from the figure that, e.g., a message with a duration of about four days would be detected with a probability of 5%.

It is easy to understand that the optimum sequence of observations to ensure the shortest possible duration of the message to be detected with a probability of 100%, should be an equidistant sequence in time. The sequence in Fig. 5 is generally not optimal from this point of view. However, it can be seen that during the 2015–2016 observing session relatively long periods occurred when observations were made daily, and the duration of the shortest message detectable with a probability of 100%, was only one day.

6. CONCLUSIONS

No signs of extraterrestrial signals of artificial origin were detected in the 2015 and 2016 observations made at RATAN-600 radio telescope.

The accumulation of data over two years of observations made it possible to perform a search for weak signals with a detection level of several mJy at centimeter-wave frequencies. The limits for the power of extraterrestrial-civilization signals averaged over the entire data set lie in the interval 10^{16}–10^{20} W, whereas the upper limits for luminosity in single observations (beam transit times of 7–19 seconds) are typically equal to 10^{17}–10^{21} W. The antenna gain for large parabolic emitters at centimeter-wave frequencies (Arecibo) can be as high as 5×10^7 and therefore the effective isotropic radiated power (EIRP) [8, 17] of hypothetical extraterrestrial transmitters cannot exceed 2×10^9–2×10^{13} W, which is close to the corresponding parameter for the largest ground-based planetary radar. An analysis of the statistics of observing sessions over two years showed that with daily sets, transmissions with a power exceeding the above limits can be detected with a probability of 100%. Finally, no radio emission from Sun-like exoplanet host stars with power exceeding the limits listed in Table 4 was detected either in individual observations or in averaged data during the entire monitoring period. Observations on RATAN-600 radio telescope within the framework of SETI program continue.

FUNDING

This work was a carried out within the framework of "Fundamental Research" government order of the Special Astrophysical Observatory of the Russian Academy of Sciences. Observations of extrasolar planets with RATAN-600 were supported by the Russian Science Foundation (grant No. 14-50-00043, ("Exoplanets" field of research). The data analysis

was supported by the Russian Foundation for Basic Research (grant No. 17-52-45048) and the Federal Program for Improving Competitiveness of Kazan (Volga River) Federal University.

CONFLICT OF INTEREST

The author declares that there is no conflict of interest regarding the publication of this article.

REFERENCES

1. G. Cocconi and P. Morrison, Nature **184**, 844 (1959).
2. F. D. Drake, Physics Today **14**, 40 (1961).
3. V. S. Troitskii, *Scientific basis of the existence of and search for extraterrestrial civilizations* (Nauka, Moscow, 1986).
4. J. C. Tarter, A. Agrawal, R. Ackermann, Proc. of the SPIE**7819**, 781902 (2010).
5. J. T. Wright, S. Kanodia, and E. Lubar, Astron. J. **156**, 260 (2018).
6. H. Isaacson, A. P. V. Siemion, G. W. Marcy, et al., Publ. Astron. Soc. Pacific **129**, 054501 (2017).
7. S. P. Worden, J. Drew, A. Siemion, et al., Acta Astronautica **139**, 98 (2017).
8. J. E. Enriquez, A. Siemion, G. Foster, et al., Astrophys. J. **849**, 104 (2017).
9. V. S. Troitskij, L. N. Bondar', and A. M. Starodubtsev, Uspekhi Fiz. Nauk **113**, 719 (1974).
10. N. S. Kardashev, V. A. Soglasnov, N. A. Savel'eva, et al., Astron. Zh. **54**, 3 (1977).
11. L. M. Gindilis, *SETI: Poisk vnezemnogo razuma* (Fizmatlit, Moscow, 2004).
12. M. Mayor and D. Queloz, Nature **378**, 355 (1995).
13. W. J. Borucki, D. Koch, G. Basri, et al., Science **327**, 977 (2010).
14. S. R. Kane, M. L. Hill, J. F. Kasting, et al., Astrophys. J. **830**, 1 (2016).
15. A. P. V. Siemion, P. Demorest, E. Korpela, et al., Astrophys. J. **767**, 94 (2013).
16. S. K. Sirothia, A. Lecavelier des Etangs, Gopal-Krishna, et al., Astron. and Astrophys. **562**, A108 (2014).
17. G. R. Harp, J. Richards, J. C. Tarter, et al., Astron. J. **152**, 181 (2016).
18. J.-L. Margot, A. H. Greenberg, P. Pinchuk, et al., Astron. J. **155**, 209 (2018).
19. B. M. Oliver and J. Billingham, eds., *Project Cyclops: A Design Study of a System for Detecting Extraterrestrial Intelligent Life* (Stanford Research Institute; United States. National Aeronautics and Space Administration. Project Cyclops; Ames Research Center. Project Cyclops, 1971).
20. A. Wandel, Int. J. Astrobiology **14**, 511 (2015).
21. E. M. Gabidulin and N. I. Pilipchuk, *Lekcii po teorii informacii* (MFTI, Dolgoprudnyj, 2007).
22. V. V. Kotel'nikov, in: *Vnezemnye tsivilizatsii*, 83 (Erevan, 1965).
23. J. M. Cordes, J. W. Lazio, and C. Sagan, Astrophys. J. **487**, 782 (1997).
24. H. Maehara, T. Shibayama, S. Notsu, et al., Nature **485**, 478 (2012).
25. M. Lingam and A. Loeb, Astrophys. J. **848**, 41 (2017).
26. N. S. Kardashev, Sov. Astron. **8**, 217 (1964).
27. A. B. Berlin, N. A. Nizhel'skii, P. G. Tsybulev, et al., Trudy IPA RAN **24**, 183 (2012).
28. O. V. Verkhodanov, B. L. Erukhimov, M. L. Monosov, et al., Preprint No. 87, SAO RAS (Spec. Astrophys. Obs. RAS, 1992)
29. L. N. Filippova and V. S. Strelnitskij, Astronomicheskij Tsirkulyar **1531**, 31 (1988).
30. ARI Data Base for Nearby Stars. ARICNS stars in the Henry Draper Catalogue (HD) or in the HD Extension (HDE), `http://wwwadd.zah.uni-heidelberg.de/datenbanken/aricns/hd.htm` (accessed 04.09.17).
31. SIMBAD Astronomical Database, `http://simbad.u-strasbg.fr/simbad/` (accessed 04.09.17).
32. The VizieR Service for Astronomical Catalogues (CDS, Strasbourg, France), `http://vizier.u-strasbg.fr/` (accessed 04.09.17).
33. NASA exoplanet archive, `https://exoplanetarchive.ipac.caltech.edu/index.html` (accessed 04.09.17).
34. The Exoplanet Data Explorer, `http://exoplanets.org/table` (accessed 04.09.17).
35. Exoplanet.eu, `http://exoplanet.eu/catalog/` (accessed 04.09.17).
36. Planetary systems, `http://www.allplanets.ru/index.htm` (accessed 04.09.17) [in Russian].
37. G. Takeda, E. B. Ford, A. Sills et.al., *Structure and Evolution of Nearby Stars with Planets II*, `http://exoplanets.astro.yale.edu/science/analysis/spocs-evol.php` (accessed 04.09.17).
38. W. E. Harris, *Catalog of parameters for Milky Way globular clusters: the database*, `http://physwww.physics.mcmaster.ca/~harris/mwgc.dat` (accessed 04.09.17).
39. M. Kendall, and A. Stuart, *Inference and Relationship*, Vol.2: *The advanced theory of statistics* (Griffin, London, 1961; Nauka, Moskow, 1973).
40. J. J. Condon, W. D. Cotton, E. W. Greisen, et al., Astron. J. **115**, 1693 (1998).
41. J. J. Condon, W. D. Cotton, E. W. Greisen, et al., *The NRAO VLA Sky Survey*, `http://www.cv.nrao.edu/nvss` (accessed 04.09.17).

Translated by A. Dambis